Preprints of the 21st IFAC World Congress (Virtual)
Berlin, Germany, July 12-17, 2020

Lyapunov-based Stability Analysis for Conveying Fluid Pipe with Nonlinear Energy Sink

Nan Duan, Yuhu Wu, Xi-Ming Sun, Chongquan Zhong, Wei Wang

Key Laboratory of Intelligent Control and Optimization for Industrial Equipment of Ministry of Education and School of Control Science and Engineering, Dalian University of Technology, Dalian 116024*, P. R. China (e-mail: dn_1607@ mail.dlut.edu.cn, wuyuhu@dlut.edu.cn, sunxm@dlut.edu.cn, zhongcq@dlut.edu.cn, wangwei@dlut.edu.cn).*

Abstract: This paper considers the stability of a conveying fluid pipe with nonlinear energy sink (NES), which is a passive vibration controller. Based on the Galerkin approximation method, the fourth-order partial differential equation (PDE) model of the conveying fluid pipe-NES system is converted into an ordinary differential equation (ODE) form. Then, based on the first order characterization of convexity and energy disturbances technique under the framework of Lyapunov stability theory, global exponential stability of the conveying fluid pipe-NES system is obtained.

Keywords: Conveying fluid pipe, nonlinear energy sink, Galerkin approximation, stability analysis, energy disturbances technique

1. INTRODUCTION

The conveying fluid pipe is widely applied in industrial field, such as the system of oil/gas transmission, heat exchange, hydraulic and so on. However, the excessive vibration of the pipe caused by the fluid velocity pulsation and lead to equipment failure.

Studies on dynamic behaviors of conveying fluid pipe have begun half a century ago by Benjamin (1962). Since then, the modeling problems of dynamics behavior of conveying fluid pipe had been extensively studied (Païdoussis and Issid, 1974; Semler and Paıdoussis, 1996). Research on the coupling between pipe and fluid shown that the natural frequencies of pipe systems are highly dependent on the velocity of the fluid, which promoted the development of the dynamic behaviors modeling problem of conveying fluid pipe (Jin and Song, 2005). Then, Guo et al. (2013) made a detailed review of the nonlinear dynamics behavior of conveying fluid pipe and provided a nonlinear model.

Based on the studies of the dynamic behaviors of conveying fluid pipe, intense study efforts have been made to control unreasonable vibration of pipes. These research are mainly divided into active control and passive control. The active control requires external force generated by the actuator such as piezoelectric crystals (Moheimani and Fleming, 2006), phononic crystals (Wang and Wang, 2018) and other methods (Preumont, 2018) to inhibit the vibration of the pipe system. Thus, sensors and energy inputs are also indispensable for the active control. These factors make the active vibration controller too complex and limit its application. Different to the active control method, more and more passive control methods are applied to absorb or dissipate the vibration energy of the mechanical structure due to its simpler and more reliable controller construction. Many passive vibration controllers have been studied decades years, such as inerter (Siami et al., 2017) and nonlinear energy sink (NES) (Gendelman et al., 2001). Especially, as an essential nonlinearity structure, the NES can engage in resonance over a very wide frequency range (Gendelman et al., 2001; Vakakis and Gendelman, 2001). Then, voluminous studies have verified the feasibility and effectiveness of NES as a vibration controller, from the theoretical and experimental perspective (Gendelman et al., 2011). Thereafter, the NES vibration controller was applied to many engineering structures, such as flexible wing (Hubbard et al., 2010), elastic string (Zulli and Luongo, 2015), pipe (Yang et al., 2014). These studies are demonstrated that the NES can act as completely and inherently broadband passive vibration controller (Silva et al., 2018). It can be efficiently and robustly absorb and dissipate the vibration energy of engineering structure with lightweight and modular structure. However, for proof process of the stability and the determination of the stability type of the conveying fluid pipe systems with the NES controller, it has not received the necessary attention of the researchers. The study about the stability at present is only the method that determines the stability and critical conditions by obtaining the eigenvalues of the linearized Jacobian matrix of the motion equation of the system (Yang et al., 2014). The method of the eigenvalues of the linearized Jacobian matrix of the dynamics system can only shows the local

⋆ This work was supported by the National Natural Science Foundation of China under Grants 61890920, 61890921 and 61773090 and Liao Ning Revitalization Talents Program under Grant XLY-C1907100 and in part by the Fundamental Research Funds for the Central Universities under Grant DUT19LAB37.

stability of the conveying fluid pipe-NES system, not the global stability as in the literature (Wu et al., 2014, 2015). Therefore, it is necessary to study the global stability of the conveying fluid pipe-NES system.

In this paper, based on the Galerkin approximation method, the fourth-order partial differential equation (PDE) model of the conveying fluid pipe-NES system is converted into a second-order ordinary differential equation (ODE) system with a nonlinear term, which is the gradient of a convex function. Then, we establish a Lyapunov function of the approximate conveying fluid pipe-NES system based on the first order characterization of convexity and energy disturbances technique by the functional analysis method. Therefore, we get that the finite dimensional approximation model of the conveying fluid pipe-NES system is global exponential stability. Finally, we verify the overall response characteristics of the conveying fluid pipe under the NES controller by a numerical simulation.

2. SYSTEM MODEL

Considering a conveying fluid pipe that is simply supported at both ends and a passive vibration controller is installed at the position D (as shown in the red dashed box in Fig. 1). The model of this system can be described by the following PDE form based on the existing research (such as Guo et al., 2013; Duan et al., 2016):

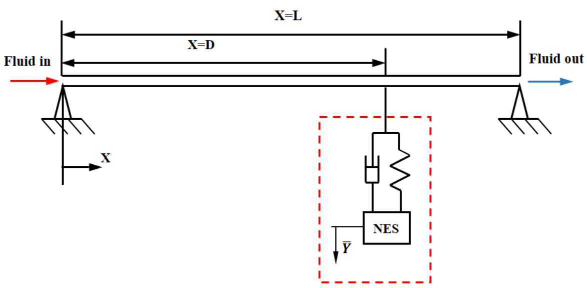

Fig. 1. Pipe conveying fluid with NES vibration controller.

$$EI\frac{\partial^4 Y(X,T)}{\partial X^4}+\lambda EI\frac{\partial^5 Y(X,T)}{\partial X^4 \partial T}+M_f V^2\frac{\partial^2 Y(X,T)}{\partial X^2} +M_f V\frac{\partial^2 Y(X,T)}{\partial X \partial T}+(M_f+m_p)\frac{\partial^2 Y(X,T)}{\partial T^2}+F(D,T)=0, \quad (1)$$

where $Y(X,T)$ is the transverse displacement of the pipe, EI is the bending stiffness of the pipe, λ is the viscoelastic coefficient of the pipe, M_f is the mass of the fluid in the pipe, the m_p is the mass of the pipe, V is the flow velocity of the fluid in the pipe, $F(D,T)$ is the control force on the conveying fluid pipe and T is the time variable, respectively.

The first term in equation (1) refer to the flexural restoring force; the second term represents the viscoelastic property of the fluid conveying pipe; the third term is relevant with the centrifugal force caused by the liquid flows; the fourth term is relevant with the Coriolis effects; the fifth term denotes the inertial force of the fluid filled pipe; and the last term is the passive control force, which means the coupling between the pipe and the controller.

According to the characteristics of the passive vibration controller, the motion equation of conveying fluid pipe can be written as follows:

$$\begin{aligned}&EI\frac{\partial^4 Y(X,T)}{\partial X^4}+\lambda EI\frac{\partial^5 Y(X,T)}{\partial X^4 \partial T}+M_f V^2\frac{\partial^2 Y(X,T)}{\partial X^2}\\&+M_f V\frac{\partial^2 Y(X,T)}{\partial X \partial T}+(M_f+m_p)\frac{\partial^2 Y(X,T)}{\partial T^2}\\&+\left\{K\left[Y(d,T)-\overline{Y}(T)\right]^3\right.\\&\left.+C\left[\frac{\partial Y(d,T)}{\partial T}-\frac{d\overline{Y}(T)}{dT}\right]\right\}\delta(X-D)=0,\end{aligned} \quad (2)$$

where the last term is the detailed form of the control force $F(D,T)$. $\overline{Y}(T)$ is the the transverse displacement of the NES vibration controller, m_{NES} is the mass of the NES, K is the nonlinear(cubic) stiffness of the vibration controller, C is the damping of the NES system, $\delta(X-D)$ is the Dirac delta function.

The motion equation of NES is

$$\begin{aligned}m_{NES}\frac{d^2\overline{Y}(T)}{dT^2}&+K\left[\overline{Y}(T)-Y(d,T)\right]^3\\&+C\left[\frac{d\overline{Y}(T)}{dT}-\frac{\partial Y(d,T)}{\partial T}\right]=0.\end{aligned} \quad (3)$$

Note that the mass of NES system is lightweight compared with the total mass of pipe and fluid, that is

$$\frac{m_{NES}}{M_f+m_p}=\varepsilon \ll 1,$$

where the ε is a small parameter. Define the following nondimensional quantities process

$$\begin{aligned}&y=\frac{Y}{L},x=\frac{X}{L},\overline{y}=\frac{\overline{Y}}{L},t=\frac{T}{L^2}\sqrt{\frac{EI}{M_f+m_p}},d=\frac{D}{L},\\&\alpha=\frac{\lambda}{L^2}\sqrt{\frac{EI}{M_f+m_p}},\beta=\frac{M_f}{M_f+m_p},\varepsilon=\frac{m_{NES}}{M_f+m_p},\\&v=VL\sqrt{\frac{M_f}{EI}},k=\frac{KL^6}{EI},\sigma=\frac{L^2C}{\sqrt{EI(M_f+m_p)}},\end{aligned} \quad (4)$$

putting them into equations (2) and (3), the dimensionless forms of conveying fluid pipe-NES system are obtained as follows:

$$\begin{aligned}&\frac{\partial^4 y(x,t)}{\partial x^4}+\alpha\frac{\partial^5 y(x,t)}{\partial x^4\partial t}+v^2\frac{\partial^2 y(x,t)}{\partial x^2}+2\sqrt{\beta}v\frac{\partial^2 y(x,t)}{\partial x\partial t}\\&\quad+\frac{\partial^2 y(x,t)}{\partial t^2}+\left\{k\left[y(d,t)-\overline{y}(t)\right]^3\right.\\&\quad\left.+\sigma\left[\frac{\partial y(d,t)}{\partial t}-\frac{d\overline{y}(t)}{dt}\right]\right\}\delta(x-d)=0,\end{aligned} \quad (5)$$

$$\begin{aligned}\varepsilon\frac{d^2\overline{y}(t)}{dt^2}&+k\left[\overline{y}(t)-y(d,t)\right]^3\\&+\sigma\left[\frac{d\overline{y}(t)}{dt}-\frac{\partial y(d,t)}{\partial t}\right]=0.\end{aligned} \quad (6)$$

3. PRETREATMENT OF SYSTEM MODEL

The model of conveying fluid pipe-nonlinear energy sink system given by (5) and (6) is a fourth-order PDE form, which needs to be transformed into an ODE form by utilizing the Galerkin approximation approach to analyze the stability of the closed-loop system more tractable. The displacement function of the closed-loop system is expanded into the following form (see Kheiri et al., 2014; Ch'ng, 1977):

$$y(x,t)=\sum_{r=1}^{n}\phi_r(x)q_r(t), \tag{7}$$

where $\phi_r(x)$ are the eigenfunctions for the free undamped vibration of a pipe conveying fluid, $q_r(t)$ are the generalized coordinates of the discretized system, and n is the number of Galerkin approximation terms.

Thus, the following theorem for this closed-loop system can be obtained.

Theorem 1. Based on the Galerkin-type projection (7), the fourth-order PDE form (5) and (6) of the conveying fluid pipe-NES system can be converted into a nonlinear autonomous system, which is a second-order ODE system

$$\boldsymbol{M}\ddot{\boldsymbol{Z}}+\boldsymbol{C}\dot{\boldsymbol{Z}}+\boldsymbol{K}\boldsymbol{Z}+\boldsymbol{F}N(\boldsymbol{Z})=0 \tag{8}$$

with

$$\begin{gathered}\boldsymbol{Z}=\begin{bmatrix}\boldsymbol{q}(t)\\ \overline{y}(t)\end{bmatrix}\in\boldsymbol{R}^{n+1},\boldsymbol{M}=\left[\begin{array}{c|c}\boldsymbol{M_0}&\boldsymbol{0}\\\hline\boldsymbol{0}&\varepsilon\end{array}\right],\boldsymbol{K}=\left[\begin{array}{c|c}\boldsymbol{K_0}&\boldsymbol{0}\\\hline\boldsymbol{0}&\boldsymbol{0}\end{array}\right],\\ \boldsymbol{C}=\left[\begin{array}{c|c}\boldsymbol{C_0}+\widetilde{\boldsymbol{C}}&\overline{\boldsymbol{C}}^T\\\hline\overline{\boldsymbol{C}}&\sigma\end{array}\right],\boldsymbol{F}=\begin{bmatrix}-k\boldsymbol{\phi_{rd}}\\k\end{bmatrix},\boldsymbol{M_0}=\boldsymbol{\delta_r},\\ \boldsymbol{C_0}=\alpha\lambda_r^4\boldsymbol{\delta_r}+2\sqrt{\beta}v\boldsymbol{b_r},N(\boldsymbol{Z})=(\overline{y}-\boldsymbol{\phi_{rd}^T}\boldsymbol{q})^3,\\ \boldsymbol{K_0}=\lambda_r^4\boldsymbol{\delta_r}+v^2\boldsymbol{c_r},\widetilde{\boldsymbol{C}}=\sigma\boldsymbol{\phi_{rd}}\boldsymbol{\phi_{rd}^T},\overline{\boldsymbol{C}}=-\sigma\boldsymbol{\phi_{rd}^T},\\ \boldsymbol{\phi_r}=\left[\,\phi_1(x)\cdots\phi_n(x)\,\right]^T,\boldsymbol{\phi_{rd}}=\left[\,\phi_1(d)\cdots\phi_n(d)\,\right]^T,\\ \boldsymbol{q_r}=\left[\,q_1(t)\cdots q_n(t)\,\right]^T,\end{gathered} \tag{9}$$

where $\boldsymbol{M}$, $\boldsymbol{C}$ and $\boldsymbol{K}$ are the mass matrix, damping matrix and stiffness matrix of the whole system, respectively. The matrices $\boldsymbol{M_0}$, $\boldsymbol{C_0}$ and $\boldsymbol{K_0}$ represent the mass, damping and stiffness of the conveying fluid pipe which is a simply supported pipe at both ends. ε and σ are the matrix of mass and damping of the controller, respectively, $\overline{\boldsymbol{C}}$ is the damping matrix associated with $\dot{\boldsymbol{q}}(t)$ in the controller, $\overline{\boldsymbol{C}}^T$ is the damping matrix associated with $\dot{\overline{y}}(t)$ in the part of pipe. N is the basic nonlinear term of the closed-loop system, $\boldsymbol{F}$ is the nonlinear coefficient of the system. $\boldsymbol{\delta_r}$, $\boldsymbol{b_r}$ and $\boldsymbol{c_r}$ are Kronecker products of $\boldsymbol{\phi_r}$ and $\boldsymbol{\phi_r}$,$\boldsymbol{b_r}$ and $\boldsymbol{c_r}$, respectively.

The detailed proof process can refer to the author's previous publication Duan et al. (2016). Now, the intractable fourth-order PDE model (5)-(6) of the conveying fluid pipe-NES system is transformed into an tractable ODE form (8).

4. STABILITY ANALYSIS

In this section, we will give stability of the conveying fluid pipe-NES system. To deduce the stability results, the potential energy function $U(\boldsymbol{Z})$ of system (8) is defined as follows

$$U(\boldsymbol{Z})=\frac{1}{2}\langle\boldsymbol{K}\boldsymbol{Z},\boldsymbol{Z}\rangle+\frac{k}{4}(\boldsymbol{\phi_{rd}^T}\boldsymbol{q}-\overline{y})^4. \tag{10}$$

where the symbol $\langle\cdot,\cdot\rangle$ denotes the Euclidean inner product of two vectors in $\boldsymbol{R}^{n+1}$. It is easy to check that $U(\boldsymbol{Z})$ is a convex function.

According to the definition (10) of $U(\boldsymbol{Z})$, nonlinear second-order autonomous model (8) can be written as the following form

$$\boldsymbol{M}\ddot{\boldsymbol{Z}}+\boldsymbol{C}\dot{\boldsymbol{Z}}+\nabla U(\boldsymbol{Z})=\boldsymbol{0}, \tag{11}$$

where $\nabla U(\boldsymbol{Z})$ represents the gradient of potential energy function $U(\boldsymbol{Z})$.

To presenting the main stability result for the system (8), we define a energy functional $E(t)$ and a disturbance functional $W(t)$ of the system based on (11), as follows:

$$E(t)=\frac{1}{2}\langle\boldsymbol{M}\dot{\boldsymbol{Z}},\dot{\boldsymbol{Z}}\rangle+U(\boldsymbol{Z}), \tag{12}$$

$$W(t)=\langle\boldsymbol{M}\dot{\boldsymbol{Z}},\boldsymbol{Z}\rangle+\frac{1}{2}\langle\boldsymbol{C}\boldsymbol{Z},\boldsymbol{Z}\rangle. \tag{13}$$

Then, for $W(t)$ we obtain that

$$W(t)\geqslant\langle\boldsymbol{M}\dot{\boldsymbol{Z}},\boldsymbol{Z}\rangle+\frac{1}{2}\lambda_{\boldsymbol{C}}^{min}\left\|\boldsymbol{Z}\right\|_2^2. \tag{14}$$

Applying the Young inequality

$$\langle\boldsymbol{X},\boldsymbol{Y}\rangle\geqslant-\frac{1}{2\theta}\left\|\boldsymbol{X}\right\|_2^2-\frac{\theta}{2}\left\|\boldsymbol{Y}\right\|_2^2,$$

with $\theta=\lambda_{\boldsymbol{C}}^{min}$, (14) can be converted into

$$\begin{aligned}W(t)&\geqslant-\frac{1}{2\lambda_{\boldsymbol{C}}^{min}}\left\|\boldsymbol{M}\dot{\boldsymbol{Z}}\right\|_2^2-\frac{1}{2}\lambda_{\boldsymbol{C}}^{min}\|\boldsymbol{Z}\|_2^2+\frac{1}{2}\lambda_{\boldsymbol{C}}^{min}\|\boldsymbol{Z}\|_2^2\\&=-\frac{1}{2\lambda_{\boldsymbol{C}}^{min}}\left\|\boldsymbol{M}\dot{\boldsymbol{Z}}\right\|_2^2\geqslant-\frac{\lambda_{\boldsymbol{M}}^{max}}{2\lambda_{\boldsymbol{C}}^{min}}\langle\dot{\boldsymbol{Z}},\boldsymbol{M}\dot{\boldsymbol{Z}}\rangle,\end{aligned} \tag{15}$$

noticing $\boldsymbol{M}$ is a diagonal matrix from (9), hence

$$W(t)\geqslant-\frac{\lambda_{\boldsymbol{M}}^{max}}{2\lambda_{\boldsymbol{C}}^{min}}\langle\dot{\boldsymbol{Z}},\boldsymbol{M}\dot{\boldsymbol{Z}}\rangle,$$

that is

$$W(t)\geqslant-\frac{\lambda_{\boldsymbol{M}}^{max}}{\lambda_{\boldsymbol{C}}^{min}}E(t). \tag{16}$$

Now, we provide the primary stability result for the conveying fluid pipe-NES system (8) based on the first order characterization of convexity and energy disturbance technique.

Theorem 2. For system (8), define a Lyapunov function

$$V(t)=E(t)+\frac{1}{\rho}W(t), \tag{17}$$

with $\rho=max\left\{\frac{\lambda_{\boldsymbol{M}}^{max}}{\lambda_{\boldsymbol{C}}^{min}},\frac{3}{2}\lambda_{\boldsymbol{MC^{-1}}}^{max}\right\}$. Then, for all $t>0$,

$$0\leqslant V(t)\leqslant V(0)e^{-\frac{1}{\rho+p}t} \tag{18}$$

where constant $p=max\left\{\frac{(\lambda_{\boldsymbol{N}}^{max})^2}{(\lambda_{\boldsymbol{C}}^{max}\lambda_{\boldsymbol{M}}^{min})},2\frac{\lambda_{\boldsymbol{C}}^{max}}{\lambda_{\boldsymbol{K}}^{min}}\right\}$, with $\lambda_{\boldsymbol{M}}^{max}$ and $\lambda_{\boldsymbol{M}}^{min}$ are the maximum and minimum eigenvalues of matrix $\boldsymbol{M}$, respectively. $\lambda_{\boldsymbol{C}}^{min}$ is the minimum eigenvalue of matrix $\boldsymbol{C}$, $\lambda_{\boldsymbol{K}}^{min}$ is the minimum eigenvalue of matrix $\boldsymbol{K}$, $\lambda_{\boldsymbol{MC^{-1}}}^{max}$ is the maximum eigenvalue of the product of matrix $\boldsymbol{M}$ and the inverse matrix of $\boldsymbol{C}$.

Proof. From (12) of the energy functional of system (8), $\dot{E}(t)$ can be deduced into the following form

$$\begin{aligned}\dot{E}(t)&=\langle\dot{\boldsymbol{Z}},\boldsymbol{M}\ddot{\boldsymbol{Z}}\rangle+\langle\dot{\boldsymbol{Z}},\nabla U(\boldsymbol{Z})\rangle=\langle\dot{\boldsymbol{Z}},\boldsymbol{M}\ddot{\boldsymbol{Z}}+\nabla U(\boldsymbol{Z})\rangle\\&=-\langle\dot{\boldsymbol{Z}},\boldsymbol{C}\dot{\boldsymbol{Z}}\rangle\leqslant-\lambda_{\boldsymbol{C}}^{min}\left\|\dot{\boldsymbol{Z}}\right\|_2^2.\end{aligned} \tag{19}$$

Next, recalling definition (13) of $W(t)$, it is straightforward to have the functional $\dot{W}(t)$ as follows:

$$\begin{aligned}\dot{W}(t)=&\langle \boldsymbol{M}\ddot{\boldsymbol{Z}},\boldsymbol{Z}\rangle+\langle \boldsymbol{M}\dot{\boldsymbol{Z}},\dot{\boldsymbol{Z}}\rangle+\frac{1}{2}\langle \boldsymbol{C}\boldsymbol{Z},\dot{\boldsymbol{Z}}\rangle+\frac{1}{2}\langle \boldsymbol{C}\dot{\boldsymbol{Z}},\boldsymbol{Z}\rangle\\ =&\langle \boldsymbol{M}\ddot{\boldsymbol{Z}}+\boldsymbol{C}\dot{\boldsymbol{Z}},\boldsymbol{Z}\rangle+\langle \boldsymbol{M}\dot{\boldsymbol{Z}},\dot{\boldsymbol{Z}}\rangle.\end{aligned} \tag{20}$$

Substituting (11) into (20), we have

$$\dot{W}(t)=-\langle \nabla U(\boldsymbol{Z}),\boldsymbol{Z}\rangle+\langle \boldsymbol{M}\dot{\boldsymbol{Z}},\dot{\boldsymbol{Z}}\rangle. \tag{21}$$

Considering $U(\boldsymbol{Z})$ is a convex function. Hence, using Theorem 25.1 in Rockafellar (2015), we can obtain that $U(\boldsymbol{Z})$ satisfies the following inequality, for all $\boldsymbol{Z}\in\boldsymbol{R}^{n+1}$,

$$\langle \nabla U(\boldsymbol{Z}),\boldsymbol{Z}\rangle\geqslant U(\boldsymbol{Z}). \tag{22}$$

Combining equation (21) and inequality (22), we have

$$\dot{W}(t)\leqslant -U(\boldsymbol{Z})+\langle \boldsymbol{M}\dot{\boldsymbol{Z}},\dot{\boldsymbol{Z}}\rangle. \tag{23}$$

Then, we obtain that $E(t)+\dot{W}(t)$ satisfies the following inequality by combining (12) and (23),

$$\begin{aligned}E(t)+\dot{W}(t)&\leqslant\frac{1}{2}\langle \boldsymbol{M}\dot{\boldsymbol{Z}},\dot{\boldsymbol{Z}}\rangle+U(\boldsymbol{Z})-U(\boldsymbol{Z})+\langle \boldsymbol{M}\dot{\boldsymbol{Z}},\dot{\boldsymbol{Z}}\rangle\\ &=\frac{3}{2}\langle \boldsymbol{M}\dot{\boldsymbol{Z}},\dot{\boldsymbol{Z}}\rangle=\frac{3}{2}\lambda^{max}_{\boldsymbol{MC}^{-1}}\langle \boldsymbol{C}\dot{\boldsymbol{Z}},\dot{\boldsymbol{Z}}\rangle,\end{aligned} \tag{24}$$

Noticing $\rho\geqslant\frac{3}{2}\lambda^{max}_{\boldsymbol{MC}^{-1}}$, and substituting (19) in (24) gets that

$$E(t)+\dot{W}(t)\leqslant-\rho\dot{E}(t),$$

that is

$$E(t)+\rho\dot{E}(t)+\dot{W}(t)\leqslant 0. \tag{25}$$

Through the Young inequality with $\theta=\lambda^{max}_{\boldsymbol{C}}$, the following inequality is obtained from (13)

$$\begin{aligned}W(t)&\leqslant\frac{\|\boldsymbol{M}\dot{\boldsymbol{Z}}\|_2^2}{2\lambda^{max}_{\boldsymbol{C}}}+\lambda^{max}_{\boldsymbol{C}}\|\boldsymbol{Z}\|_2^2\\ &\leqslant\frac{1}{2}\frac{(\lambda^{max}_{\boldsymbol{M}})^2}{\lambda^{max}_{\boldsymbol{C}}}\|\dot{\boldsymbol{Z}}\|_2^2+\lambda^{max}_{\boldsymbol{C}}\|\boldsymbol{Z}\|_2^2.\end{aligned} \tag{26}$$

where $\lambda^{max}_{\boldsymbol{C}}$ is the maximum eigenvalue of the matrix $\boldsymbol{C}$. According to definition (10) of the potential energy function $U(\boldsymbol{Z})$, we deduce that

$$U(\boldsymbol{Z})\geqslant\frac{1}{2}\lambda^{min}_{\boldsymbol{K}}\|\boldsymbol{Z}\|_2^2. \tag{27}$$

Therefore, energy functional $E(t)$ satisfies

$$E(t)\geqslant\frac{1}{2}\lambda^{min}_{\boldsymbol{M}}\|\dot{\boldsymbol{Z}}\|_2^2+\frac{1}{2}\lambda^{min}_{\boldsymbol{K}}\|\boldsymbol{Z}\|_2^2. \tag{28}$$

Then, there is a positive real number p that satisfies

$$\frac{1}{2}p\lambda^{min}_{\boldsymbol{M}}\geqslant\frac{1}{2}\frac{(\lambda^{max}_{\boldsymbol{M}})^2}{\lambda^{max}_{\boldsymbol{C}}},\ \frac{1}{2}p\lambda^{min}_{\boldsymbol{K}}\geqslant\lambda^{max}_{\boldsymbol{C}},$$

such that

$$W(t)\leqslant pE(t) \tag{29}$$

The first term of inequality (25) can be decomposed into $(1-s)E(t)+sE(t)$, where $s\in[0,1]$. And by using the relationship (29) between $W(t)$ and $E(t)$, inequality (25) can be written as follows

$$(1-s)E(t)+\frac{s}{p}W(t)+\rho\dot{E}(t)+\dot{W}(t)\leqslant 0, \tag{30}$$

which can be further factorized into the following form

$$\begin{aligned}&(1-s-\frac{s\rho}{p})E(t)+\frac{s\rho}{p}\left[E(t)+\frac{1}{\rho}W(t)\right]\\ &+\rho\left[\dot{E}(t)+\frac{1}{\rho}\dot{W}(t)\right]\leqslant 0.\end{aligned} \tag{31}$$

Now, set $s=\frac{p}{p+\rho}$, which implies $1-s-\frac{s\rho}{p}=0$. Thus,

$$\frac{\rho}{\rho+p}\left[E(t)+\frac{1}{\rho}W(t)\right]+\rho\left[\dot{E}(t)+\frac{1}{\rho}\dot{W}(t)\right]\leqslant 0. \tag{32}$$

which can be rewritten as $V(t)/(\rho+p)\leqslant-\dot{V}(t)$, by recalling definition of Lyapunov function given in (17). Therefore, we obtain

$$V(t)\leqslant V(0)e^{-\frac{1}{\rho+p}t} \tag{33}$$

By applying (16), the Lyapunov function $V(t)$ satisfies

$$V(t)=E(t)+\frac{1}{\rho}W(t)\geqslant(1-\frac{1}{\rho}\frac{\lambda^{max}_{\boldsymbol{M}}}{\lambda^{min}_{\boldsymbol{C}}})E(t). \tag{34}$$

Notice $\rho=\frac{3}{2}max\left\{\frac{\lambda^{max}_{\boldsymbol{M}}}{\lambda^{min}_{\boldsymbol{C}}},\lambda^{max}_{\boldsymbol{MC^{-1}}}\right\}$, we have $0<1-\frac{1}{\rho}\frac{\lambda^{max}_{\boldsymbol{M}}}{\lambda^{min}_{\boldsymbol{C}}}<1$. Recalling the definition (12), we obtain that $E(t)\geqslant 0$. Therefore, $V(t)$ satisfies that

$$V(t)\geqslant 0. \tag{35}$$

By combining (33) and (35), we obtain inequality (18), and the proof of Theorem 2 is completed. □

Inequalities (18) and (34) in the prove process of Theorem 2, we obtain the following corollary.

Corollary 3. Let $\kappa=V(0)/\left(1-\frac{1}{\rho}\frac{\lambda^{max}_{\boldsymbol{M}}}{\lambda^{min}_{\boldsymbol{C}}}\right)$, then the energy functional $E(t)$ satisfies

$$0\leqslant E(t)\leqslant\kappa e^{-\frac{1}{\rho+p}t},\quad \text{for all } t>0, \tag{36}$$

where $V(0)$ and ρ are given in Theorem 2.

Remark 4:

(1) Lyapunov-based stability criterion (18) of the system (8) is obtained during Theorem 2. It is illustrated that the function $V(t)$ exponentially tends to zero.
(2) Combining (36) in Corollary 3 and (18) in Theorem 2 it is demonstrated that the energy functional $E(t)$ also obeys the exponential convergence condition. In other words, the vibration energy of approximation system (8) is dissipated by the NES to zero in an exponent form.

Theorem 2 and Corollary 3 show that the conveying fluid pipe-NES system (5)-(6) is globally exponentially stable.

5. SIMULATION RESULTS

In this section, we will discuss a computational simulation example to validate the stability proof results of conveying fluid pipe-NES system in Section 3. The system model was firstly transformed into an ODE form from a fourth-order PDE form (5)- (6) during Galerkin method. No analytic solutions are available to get the transient dynamics. Therefore, it must be rely on the numerical methods. The Galerkin method in Section 3 can be well approximated the amplitude of the displacement $y(x,t)$ (see Yang et al., 2014; Nechak et al., 2017). Many studies (such as Holmes, 1978; Javadi et al., 2019) have shown that two-order approximation of equation (7) can ensure its sufficient accuracy for the conveying fluid pipe simply supported at both ends. So we take three-term Galerkin approximation, that is $n=3$ in (7) in this section. The initial conditions of simulation examples are

$$\dot{q}_1(0)=A,\quad q_1(0)=\dot{q}_2(0)=q_2(0)=\dot{q}_3(0)=q_3(0)=0,$$
$$\dot{\bar{y}}(0)=\bar{y}(0)=0$$

where a is a constant. And, the boundary conditions of the conveying fluid pipe are

$$y(0,t) = \dot{y}(0,t) = 0, y(1,t) = \dot{y}(1,t) = 0.$$

The simulation parameters of conveying fluid pipe and NES are shown in table 1.

Table 1. The system parameters in simulation

Parameter	Description	Value
α	The dimensionless viscoelastic coefficient of pipe	0.001
β	The mass ratio of the mass of fluid in pipe and the total mass of fluid and pipe	0.8
ε	The mass ratio of the controller and the total mass of the system	0.1
σ	The dimensionless damping of the controller	0.1
k	The dimensionless stiffness of the controller	8000
d	The dimensionless installation location of the controller	0.4
v	The dimensionless velocity of fluid in pipe	2
A	The initial distributed velocity in simulations	0.3

Based on the above initial conditions, boundary conditions and system parameters, we first show the vibration control effective of NES.

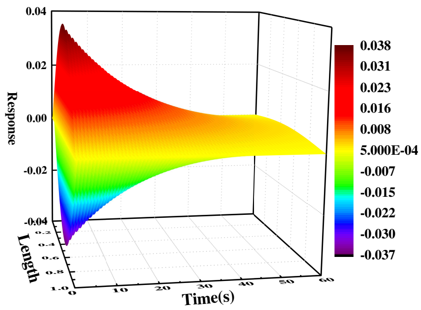

(a) *without NES*

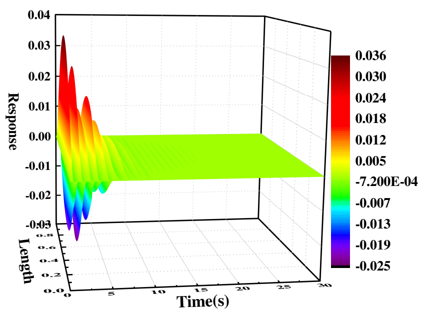

(b) *with NES*

Fig. 2. The displacement response $y(x,t)$ of the pipe under different conditions at fluid velocity $v = 2$.

The vibration control effective of NES is intuitive validated by some simulation. Fig. 2(a) show the displacement $y(x,t)$ of the pipe without control at fluid velocity $v = 2$. The result shows that the peak of response after 60s (0.0022) is still 5.8% of the maximum peak (0.0384). This illustrates that the pipe is difficult to reach a steady state after being excited. The displacement response of the pipe with

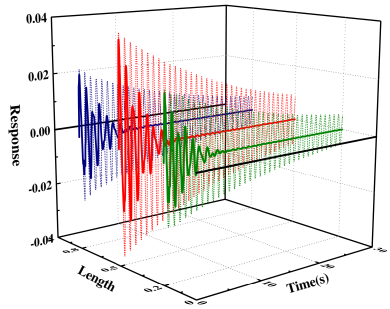

Fig. 3. Visualized comparison of several section displacement response of the conveying fluid pipe under different conditions at $v = 2$.

NES as a comparison is shown in Fig. 2(b). Based on the numerical results, we obtain that the peak response (0.00164) of the pipe has decayed to less than 5% of the maximum peak (0.036) after 8.1s and the maximum peak response is also reduced by 6.25% (0.0384 to 0.036). These results manifests that the introduction of NES not only accelerate the pipe to reach a steady state but also reduce the maximum response peak of it. In addition, to explain the vibration control effect of NES more intuitively, we compared the displacement of several sections as shown in Fig. 3. In Fig. 3, the color of the line is used to distinguish different sections (green line is $x = 0.2$, red line is $x = 0.5$ and blue line is $x = 0.8$) and apply line type to indicate different conditions (dotted lines denote the response of pipe without control and the solid lines are the response of it with NES).

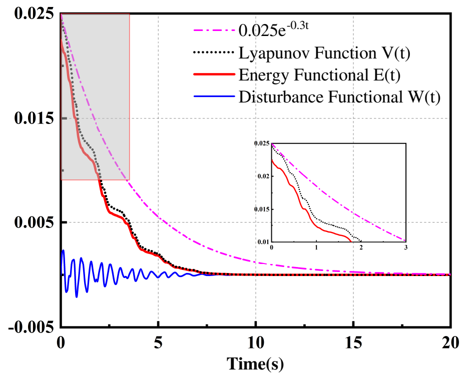

Fig. 4. $V(t)$, $E(t)$ and $W(t)$ of the conveying fluid pipe-NES system at fluid velocity $v = 2$.

Then, to explain the fast convergence of the displacement response (as showed in Fig. 2(b) and the solid lines in Fig. 3), the stability in Section 4 will be examined intuitively and analyzed during numerical simulation. Fig. 4 shows the simulation results of the energy functional $E(t)$, disturbance functional $W(t)$ and Lyapunov function $V(t)$ of system (8), which are built in Section 4. It is easy to get the following results from Fig. 4:

(1) Verification of Theorem 2. Based on the hypotheses in Theorem 2, an exponential function (such as $0.025e^{-0.3t}$) can be easily built as shows by the purple dot dash line in Fig. 4. And, it can intuitively get $0 \leqslant V(t) \leqslant 0.025e^{-0.3t}$ through the simulation results, and as the black dotted line and the purple

dot dash line in Fig. 4. That is, the Lyapunov function $V(t)$ exponentially tends to 0.

(2) Verification of Corollary 3. It is easy to obtain that $0 \leqslant E(t) \leqslant V(t)$ from Fig. 4 and its partial enlarged view (see the red solid line and the black dotted line). Namely, the energy functional of the conveying fluid pipe-NES system also satisfies $0 \leqslant E(t) \leqslant 0.025e^{-0.3t}$.

(3) It shows that $V(t)$ and $E(t)$ exponentially tend to 0 as $t > 0$. After 9 seconds, $E(t)$ and $V(t)$ are very close to 0 ($E(9) = 2.84 \times 10^{-5}$ is $\frac{1}{792}$ of $E(0) = 0.0225$ and $V(9) = 2.8442 \times 10^{-5}$ is $\frac{1}{868}$ of $V(0) = 0.0247$).

These simulation results visually verify the stability. That is, the approximation system (8) is exponential stability.

6. CONCLUSION

In this paper, we first proved that global stability of the conveying fluid pipe-NES system with finite dimensional approximation was exponentially stable. In order to achieve the stability, the Galerkin approximation approach was used to convert the fourth-order PDE model into a standard nonlinear autonomous form. Then, energy and disturbance functionals of the approximation system were carefully constructed relied on a convex function related to this system. The global exponential stability of the approximate conveying fluid pipe-NES model was obtained based on the first-order character of the convexity and energy disturbances technique under the framework of Lyapunov stability theory. Combining the Galerkin approximation approach and Remark 4, it can know that the vibration energy of the original system decays exponentially, that is, the conveying fluid pipe-NES system can be regard as exponentially stable. Finally, numerical simulations were used to verify the results of theoretical.

REFERENCES

Benjamin, T.B. (1962). Dynamics of a system of articulated pipes conveying fluid-i. theory. *Proc. R. Soc. Lond. A*, 261(1307), 457–486.

Ch'ng, E. (1977). A theoretical analysis of nonlinear effects on the flutter and divergence of a tube conveying fluid. Technical report, Princeton Univ Nj Dept of Aerospace and Mechanical Sciences.

Duan, N., Fang, B., and Teng, Y. (2016). Passive vibration control of pipes conveying fluid with parallel nonlinear energy sinks. *DEStech Transactions on Computer Science and Engineering*, (iccae).

Gendelman, O., Manevitch, L., Vakakis, A.F., and Mcloskey, R. (2001). Energy pumping in nonlinear mechanical oscillators: Part idynamics of the underlying hamiltonian systems. *Journal of Applied Mechanics*, 68(1), 34–41.

Gendelman, O.V., Sapsis, T., Vakakis, A.F., and Bergman, L.A. (2011). Enhanced passive targeted energy transfer in strongly nonlinear mechanical oscillators. *Journal of Sound and Vibration*, 330(1), 1–8.

Guo, C., Zhang, C., and Païdoussis, M. (2013). Modification of equation of motion of fluid-conveying pipe for laminar and turbulent flow profiles. In *Seismic Safety Evaluation of Concrete Dams*, 221–237. Elsevier.

Holmes, P. (1978). Pipes supported at both ends cannot flutter. *Journal of Applied Mechanics*, 45(3), 619–622.

Hubbard, S.A., Mcfarland, D.M., Bergman, L.A., and Vakakis, A.F. (2010). Targeted energy transfer between a model flexible wing and nonlinear energy sink. *J. Aircraft*, 47(6), 1918–1931. doi:10.2514/1.C001012.

Javadi, M., Noorian, M., and Irani, S. (2019). Primary and secondary resonances in pipes conveying fluid with the fractional viscoelastic model. *Meccanica*, 1–18.

Jin, J. and Song, Z. (2005). Parametric resonances of supported pipes conveying pulsating fluid. *Journal of Fluids and Structures*, 20(6), 763–783.

Kheiri, M., Païdoussis, M., Del Pozo, G.C., and Amabili, M. (2014). Dynamics of a pipe conveying fluid flexibly restrained at the ends. *Journal of Fluids and Structures*, 49, 360–385.

Moheimani, S.R. and Fleming, A.J. (2006). *Piezoelectric transducers for vibration control and damping*. Springer Science & Business Media.

Nechak, L., Raynaud, H., and Kulcsár, C. (2017). Intrusive galerkin projection for model order reduction of uncertain linear dynamic systems. *IFAC-PapersOnLine*, 50(1), 2738–2743.

Païdoussis, M.P. and Issid, N. (1974). Dynamic stability of pipes conveying fluid. *Journal of Sound and Vibration*, 33(3), 267–294.

Preumont, A. (2018). *Vibration control of active structures: an introduction*, volume 246. Springer.

Rockafellar, R.T. (2015). *Convex analysis*. Princeton university press.

Semler, C. and Paıdoussis, M. (1996). Nonlinear analysis of the parametric resonances of a planar fluid-conveying cantilevered pipe. *Journal of Fluids and Structures*, 10(7), 787–825.

Siami, A., Cigada, A., Karimi, H., Zappa, E., and Sabbioni, E. (2017). Using inerter-based isolator for passive vibration control of michelangelos rondanini pietà. *IFAC-PapersOnLine*, 50(1), 13372–13377.

Silva, T.M., Clementino, M.A., De Marqui Jr, C., and Erturk, A. (2018). An experimentally validated piezoelectric nonlinear energy sink for wideband vibration attenuation. *Journal of Sound and Vibration*, 437, 68–78.

Vakakis, A.F. and Gendelman, O. (2001). Energy pumping in nonlinear mechanical oscillators: part iiresonance capture. *Journal of Applied Mechanics*, 68(1), 42–48.

Wang, Y.Z. and Wang, Y.S. (2018). Active control of elastic wave propagation in nonlinear phononic crystals consisting of diatomic lattice chain. *Wave Motion*, 78, 1–8.

Wu, Y., Xue, X., and Shen, T. (2014). Absolute stability of the kirchhoff string with sector boundary control. *Automatica*, 50(7), 1915–1921.

Wu, Y., Xue, X., and Shen, T. (2015). Absolute stability of the axially moving kirchhoff string with a sector boundary feedback control. *Nonlinear Dynamics*, 80(1-2), 9–22.

Yang, T.Z., Yang, X.D., Li, Y., and Fang, B. (2014). Passive and adaptive vibration suppression of pipes conveying fluid with variable velocity. *Journal of Vibration and Control*, 20(9), 1293–1300.

Zulli, D. and Luongo, A. (2015). Nonlinear energy sink to control vibrations of an internally nonresonant elastic string. *Meccanica*, 50(3), 781–794.